# Evaluation of Active Appearance Models for Cardiac MRI

Tobias Böhler[1], Tobias Boskamp[1], Heinrich Müller[2],
Anja Hennemuth[1] and Heinz-Otto Peitgen[1]

[1]MeVis - Center for Medical Diagnostic Systems and Visualization,
Universitätsallee 29, 28359 Bremen
[2]LS VII Computer Graphics, University of Dortmund,
Otto-Hahn-Strasse 16, 44221 Dortmund
Email: boehler@mevis.de

**Abstract.** Robust delineation of short-axis cardiac magnetic resonance images (MRI) is a fundamental precondition for functional heart diagnostics. Segmentation of the myocardium and the left ventricular blood pool allows for the analysis of important quantitative parameters. Model-based segmentation methods based on representative image data provide an inherently stable tool for this task. We present an implementation and evaluation of 3-D Active Appearance Models for the segmentation of the left ventricle using actual clinical case images. Models created from varying random data sets have been evaluated and compared with manual segmentations.

## 1 Introduction

Cardiac Magnetic Resonance Imaging (MRI) has become a reliable method for the detection of common heart diseases. Cardiac dysfunctions, most notably the coronary heart disease, are the major cause of death in European countries and worldwide [1]. A thorough functional analysis can provide valuable data for cardiac diagnosis and therapeutical treatment planning. Fundamental parameters include the ejection fraction, the stroke volume, and the myocardial wall thickness. The computation of these values requires the delineation of the left ventricular myocardium.

The segmentation of these structure in MR images is a complex task. A variety of approaches have been proposed, which can be roughly divided into semi-automatic and fully-automatic segmentation techniques. The former include algorithms requiring a great amount of manual interaction, such as the tracing of ventricular contours using intelligent scissors [2]. If huge amounts of image data need to be processed, these methods are cumbersome. Therefore, an automation of the procedure is highly desired, and approaches using deformable models or similar model-based criteria are common. Due to noise and artifacts in MR images, model-based approaches providing inherent information on anatomical structure are highly beneficial. For instance, Active Contour

Models use image gradient forces and internal energy terms to determine contour points via a local optimization scheme [3]. For 3-D images, this technique has been extended to higher dimensional "Balloon"segmentation methods [4]. However, the gradient image required for the edge detection is often perturbed by noise and image artifacts, causing unsatisfactory segmentation results. Other approaches combine known segmentation results to a single statistical model. The segmentation is then performed by iteratively fitting the model to an input image via an optimization process. For geometrical information, this approach has found wide usage in the form of Active Shape Models, which have been applied to ventricular anatomy [5, 6]. Atlas-based segmentation methods utilize an atlas built from a training set of patient images, representing common features among those images [7]. Active Appearance Models (AAM) combine a model of the shape structure with a model of gray value intensities and have been used in a variety of applications [8]. Due to the more complex nature of the AAM, most implementations were restricted to a two-dimensional approach. Recently, the application of a full 3-D AAM to cardiac MRI and ultrasound was proposed [9]. Such approaches to cardiac functional analysis are subject to current research, and several implementations and enhancements have been reported [10]. We modified the approach of Mitchell *et al.* [9] and evaluated our implementation using a random set of cardiac images taken from actual clinical routine.

## 2 Model Generation

The creation of a single model of cardiac appearance requires a preceding delineation of the endo- and epicardial borders of the myocardium. After tracing the contours semi-automatically using intelligent scissors [2], a Procrustes analysis is performed on the set of points, registering the shapes to a common reference frame via the Iterative Closest Point (ICP) algorithm [11]. The model parameterization is computed by creating a statistical model of the shape and texture variation in the sense of a single Point Distribution Model (PDM) of shape and texture dispersions [8]. A Principle Component Analysis (PCA) is employed for this purpose [5]. In order to build a combined AAM, the PCA is applied three times. First, a model of the shape variance is constructed from the registered contour points. Subsequently, the texture model is generated by warping the textures enclosed by the outlined contours to a common reference frame, typically the mean shape, and applying the PCA once again. Finally, the combined model is constructed by creating combined parameter vectors

$$\mathbf{b_c} = \begin{pmatrix} \mathbf{W}\mathbf{c_s} \\ \mathbf{c_g} \end{pmatrix} = \begin{pmatrix} \mathbf{W}\mathbf{P_s}(\mathbf{x} - \bar{\mathbf{x}}) \\ \mathbf{P_g}(\mathbf{g} - \bar{\mathbf{g}}) \end{pmatrix}, \tag{1}$$

and performing the PCA once more, where $\mathbf{P}_g$ and $\mathbf{P}_s$ denote the corresponding eigenmatrices for shape and gray values, $\bar{\mathbf{x}}$ and $\bar{\mathbf{g}}$ give the population means, and $\mathbf{W}$ is a suitable matrix describing the correlation of gray values and textures [8]. Inverting these linear equations, corresponding model instances are constructed independently of each other. An exemplary generated shape model can be seen in Figure 1.

**Fig. 1.** Ventricular shape model (l.) and its application: Initial (m.), converged (r.).

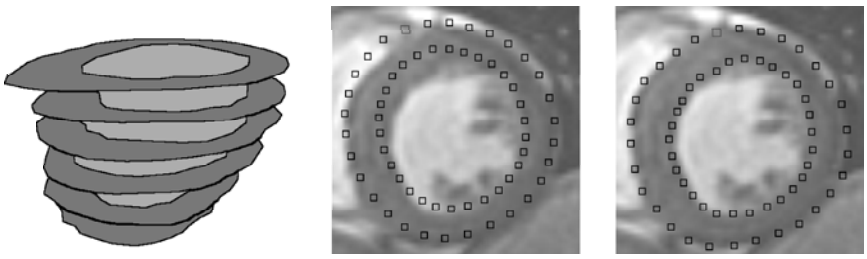

## 3 Model Fitting

The process of segmentation can be interpreted as a non-linear optimization problem of fitting the multi-parametric heart model to the input image to be processed. The difference is measured by the root mean square error

$$e(\mathbf{w}, \mathbf{g}) = (\frac{1}{n}\sum_{i=1}^{n}(w_i - g_i)^2)^{\frac{1}{2}}, \tag{2}$$

where $\mathbf{w}$ denotes the vector of warped gray values from the input image, and $\mathbf{g}$ the model gray value vector. A semi-3-D steepest descent optimization strategy is employed, using the numerically computed derivatives of the error measure and providing a stable algorithm. Transformation parameters are evaluated in directions orthogonal to the heart's long axis. The warping step is performed in a 2-D piecewise-affine fashion, computing the triangle $\Delta = (\mathbf{t}_1, \mathbf{t}_2, \mathbf{t}_3)$ containing each point $\mathbf{p} = (p_x, p_y)^T$ and solving for its barycentric coordinates $\alpha$, $\beta$, and $\gamma$ defined by $\alpha\mathbf{t}_1 + \beta\mathbf{t}_2 + \gamma\mathbf{t}_3 = \mathbf{p}$. Although this takes advantage of the layered structure of the resampled image, the loss of three-dimensional information results in an error that can not be eliminated completely. On the other hand, this allows the computation of the derivatives at running time, in contrast to the usage of a pregenerated approximation computed from a training set [5]. An initialization of the mean model instance is provided by manually positioning the contour and adjusting its scale and translation. One single image slice and the corresponding segmentation can be seen in Figure 1.

## 4 Image Data and Evaluation

The model generation described above was performed using actual clinical routine images. Three types of MR devices manufactured by General Electric (*Genesis Signa*), Philips (*Gyroscan Intera*), and Siemens (*MAGNETOM Sonata*) were used for the MRI acquisition. The image sets contained 30 anonymized dynamic images, with each image consisting of 6 to 12 different image slices. Spatial planar resolution was $256 \times 256$ voxels for most images. In the preprocessing step, these images were resampled to a common number of slices, with resulting voxel sizes

**Table 1.** Minimum and maximum distance error measures for the five models.

| Distance (mm) | $M10$ | $M15$ | $M20$ | $M25$ | $M28$ |
|---|---|---|---|---|---|
| Minimum | 0.08 | 0.11 | 0.22 | 0.24 | 0.31 |
| Maximum | 64.53 | 13.04 | 8.23 | 10.12 | 9.82 |

**Table 2.** Timings and numbers of iterations for the reference segmentations.

| | Computation time in sec. | | | Iteration steps | |
|---|---|---|---|---|---|
| Model | Average | Minimum | Maximum | Minimum | Maximum |
| $M10$ | 81.14 | 37.94 | 157.85 | **3** | 13 |
| $M15$ | 99.84 | 60.17 | 195.99 | 4 | 10 |
| $M20$ | 92.74 | 23.40 | 189.98 | **3** | 10 |
| $M25$ | 96.25 | 32.57 | 163.78 | 4 | 11 |
| $M28$ | 101.62 | 46.12 | 181.20 | **3** | 11 |

ranging from 1.7mm to 1.9mm. Short-axis two-chamber views of the left and right ventricle were selected, and the corresponding endocardial and epicardial contours were delineated manually.

Five models have been generated, with 10 to 28 images used for the model generation routine, respectively. The required images were selected randomly from the pool of existing image data, the explainable variance was set to 98% of the total variance. The accuracy of the models was determined by computing the averaged root mean square error (RMS) between manual segmentations and automatically delineated myocardial contours, as well as the minimum and maximum distance. For all models, the average segmentation error was 3.06mm (minimum 1.84mm, maximum 6.91mm). This corresponds to error distances of approximately 1.5 to 4 voxels, depending on the actual voxel size. As can be seen in Table 1, the minimum and maximum error values for the generated models ($M10$ to $M28$) vary with the number of included model images. By increasing the number of training images, the maximum error is being reduced, whereas the minimum error is being increased slightly, probably due to the greater amount of model variation. Three clinical images contained visible deformations of the myocardium, for instance dilated cardiomyopathy. The impact of these pathological images on the model-based segmentation was examined separately by creating a further Appearance Model. However, the effect of the inclusion of such images was found to be considerably low.

Since an ordinary gradient descent optimization scheme was employed, the efficiency was rather limited. Table 2 shows the average number of required iteration steps to reach convergence, as well as the average time elapsed. The computation was performed using an ordinary personal computer (1.7GHz, 2GB RAM). As can be seen from the table, an increased number of model images leads to a reduced number of iterations in some cases. In comparison to optimization methods using precomputations, the method of directly evaluating the derivatives in each iteration is more time-consuming. However, since the training set descent matrix is just an approximation, the direct method is more robust.

## 5 Discussion

We have presented an evaluation of a 3-D Active Appearance Model segmentation for the automatic delineation of cardiac anatomy. The implemented method was analyzed using random sets of actual routine clininal case images for model generation and testing. In this way a considerably high level of authenticity and a realistic assessment of the method are achieved. The evaluation results hold promise for a fully automatic model-based segmentation method, and demonstrate that the quality of the resulting segmentations depends essentially on the number of images used for the model generation. This underlines the importance of large image databases as a precursor for a plausible model generation. The results indicate that the model-based segmentation has to be combined with an efficient and intuitive correction mechanism and a more efficient optimization strategy to find its way into clinical routine image processing.

**Acknowledgements.** We would like to thank the clinical partners of the VICORA research project for providing the cardiac MR image data.

## References

1. World Health Organization. The Atlas of Heart Disease and Stroke; 2004. Available from: http://www.who.int/cardiovascular_diseases/resources/atlas/en/
2. Mortensen EricN, Barrett WilliamA. Intelligent Scissors for Image Composition. In: Proc. of SIGGRAPH. New York, NY, USA: ACM Press; 1995. p. 191–198.
3. Kass M, Witkin A, Terzopoulos D. Snakes – Active Contour Models. International Journal of Computer Vision 1987;1(4):321–331.
4. Cohen LD. On Active Contour Models and Balloons. Comput Vision Image Understand 1991;53(2):211–218.
5. Cootes TF, Taylor CJ, Cooper DH, *et al.* Active Shape Models – their Training and Application. Comput Vision Image Understand 1995;61:38–59.
6. Frangi AF, Rueckert D, Schnabel JA, *et al.* Automatic Construction of Multiple-object Three-dimensional Statistical Shape Models: Application to Cardiac Modeling. IEEE Trans Med Imaging 2002;21(9):1151–1166.
7. Lorenzo-Valdes M, Sanchez-Ortiz GI, Elkington A, *et al.* Segmentation of 4D Cardiac MR Images using a Probabilistic Atlas and the EM Algorithm. Medical Image Analysis 2004;8(3):255–265.
8. Cootes TF, Edwards GJ, Taylor CJ. Active Appearance Models. Lecture Notes in Computer Science 1998;1407:484.
9. Mitchell SC, Bosch JG, Lelieveldt BPF, *et al.* 3-D Active Appearance Models: Segmentation of Cardiac MR and Ultrasound Images. IEEE Trans Med Imaging 2002;21:1167–1178.
10. Stegmann MB, Pedersen D. Bi-temporal 3D Active Appearance Models with Applications to Unsupervised Ejection Fraction Estimation. In: Proc. SPIE Medical Imaging. SPIE; 2005.
11. Besl PJ, McKay ND. A Method for Registration of 3-D Shapes. IEEE Trans Pattern Analysis Mach Intel 1992;14(2).